CHAPTER 1
PIGEONPEA GROWTH AND DEVELOPMENT AS SIMULATED BY THE CSM-CROPGRO MODEL

1.1 Introduction

Pigeonpea (*Cajanus cajan* (L.) Millsp.) is a well-established crop in the semi-arid tropics used for food, fodder, firewood, and green manure. The development of cultivars better adapted to temperate environments is further extending the reach of this important crop (Chauhan et al., 2002). Despite its global importance, only the Agricultural Production Systems Simulator (APSIM) modeling group has developed a model for simulating pigeonpea growth (Carberry et al., 2001; Ranganathan et al., 2001; Robertson et al., 2001a,b). While appropriate for certain applications, this model lacks detail in its simulation of certain physiological processes.

The CSM-CROPGRO model is a detailed, process-based model of crop growth and development that simulates basic biological processes, such as photosynthesis and nitrogen fixation. Species, ecotype, and cultivar parameters governing various aspects of crop growth and development are stored in external parameter files. Because these parameters are separate from the model source code, CROPGRO can be readily adapted for new species without changing the existing source code. Though originally developed for use with grain legumes, it has been subsequently adapted for a number of legume and non-legume species including soybean (*Glycine max* L.), peanut (*Arachis hypogea* L.), dry bean (*Phaseolus vulgaris* L.), faba bean (*Vicia faba* L.), cotton (*Gossypium hirsutum* L.) and tomato (*Lycopersicon esculentum* Millsp.) (Boote et al., 1998a,b, 2002; Boote and Scholberg, 2006; Pathak et al., 2012; Scholberg et al., 1997). A further advantage of utilizing CROPGRO for crop growth simulation is its integration into the Cropping System Model (CSM) of the Decision Support System for Agrotechnology Transfer (DSSAT). The DSSAT-CSM includes other crop models, such as the CERES family of models (Jones et al., 2003), as well as an adaptation of the CENTURY soil organic matter model (Gijsman et al., 2003). This unique combination

of models allows for realistic long-term simulation of crop and soil dynamics for more comprehensive assessment of cropping system sustainability. The objective of this study was to adapt the CSM-CROPGRO model for simulating pigeonpea growth and development through parameter modification.

1.2 Materials and Methods

1.2.1 Data set

Model adaptation in this study was based on two primary data sets. The first was a combined field and pot study conducted at the University of Florida, Gainesville, Florida (29.7°N, 82.3°W) in 1984. The field component of the study evaluated physiological effects of water stress on several grain legumes, of which pigeonpea (cv. *76W*) was one. Only the irrigated treatment was used for parameter optimization in this study because many of the parameters are defined for non-limiting conditions. The rain-fed treatment data were used during model evaluation after parameter optimization was complete. The pot study evaluated the initial vegetative growth and partitioning of the same species. The pigeonpea was planted at a density of 11.8 plants $m^{-2}$and an initial fertilization of 40:35:130 kg $ha^{-1}$of N:P:K was applied. Plant samples were taken at 7-day intervals throughout the growing season. Leaf area index, main stem node number, and reproductive phenological stages were recorded and dry matter accumulation and N concentration for leaves, stems, pods and seeds were determined. Soil profile input data for the experiment are summarized in Table 1-1. The Soil Conservation Service curve number (SLRO) and soil photosynthesis factor (SLPF) values used were 66.0 and 0.92, respectively. Further experimental details are given in Devries et al. (1989a), Devries et al. (1989b) and Maliro (1987).

The second data set comes from a soybean-pigeonpea intercropping experiment conducted at the National Research Centre for Soybean, Indore, Madhya Pradesh, India (22.4°N, 75.5°E) in 2003-2004. Data from the sole pigeonpea treatment was used in the present study. The pigeonpea (cv. *ICPL 88039*) was planted at a density of 45 plants

m^{-2}in June 2003 and a basal dose of 20:60:20 kg $ha^{-1}$of N:P:K was applied. A single 50-mm irrigation was applied in October 2003. Plant samples were taken approximately bi-weekly from emergence to final harvest. Reproductive phenological stages were recorded and total shoot and grain dry matter were determined. Harvest index, seeds per pod, and mass per seed were determined at harvest in January 2004. Soil profile input data for the experiment is summarized in Table 1-2. SLRO and SLPF values used were 70.0 and 0.88.

1.2.2 Literature-Based Parameter Modification

CROPGRO parameter values for soybean were used as a starting point for setting parameter values for pigeonpea. Where well-established literature values existed or insufficient data was available for optimization, parameters were set based on literature values. The parameters modified based on literature are shown in Table 1-3 and include base and optimum temperatures for phenological development, tissue composition parameters, and early leaf area dynamics. The values for these parameters and the corresponding literature citations are given in Table 1-4.

The remaining parameter values requiring modification were set using parameter optimization. Descriptions of these parameters are given in Table 1-5. This process involved grouping the parameters according to their functions within the model (i.e. which model output variables they most strongly affect). This was done to prevent the implicit weighting of certain data types that had a higher number of observations than other data types. By grouping these parameters by output variable, it allowed better fitting of parameters to data. Optimization was then completed sequentially by group (i.e. the first group was optimized before the second, the second before the third, etc.). The parameters and their groupings are shown in Table 1-6. The order of parameter groupings was based on the degree of dependence on other parameters, with least dependent parameters being optimized first. This was done because the optimal values of some parameters is highly dependent on the value of other parameters. For

example, the value of EM-FL, the parameter controlling the time between emergence and flowering, is dependent on the value of PL-EM, the parameter controlling the time between planting and emergence. Crop data used for optimization from the 1984 Gainesville, FL data set are also shown by group in Table 1-6. Once these parameters had been optimized, the species parameter values were fixed and the India data set was used to optimize cultivar and ecotype parameters for *ICPL 88039*. (Table 1-8).

1.2.3 Parameter Optimization Algorithm

Parameter values were optimized using a hybrid algorithm incorporating a Gibbs-sampler (Casella and George, 1992) within a version of the Metropolis-Hastings algorithm (Chib and Greenberg, 1995). Essentially, the algorithm consists of generating vectors of candidate parameter values and evaluating them with following log-likelihood equation:

$$\ln(\mathrm{L}(\Theta_\mathrm{k}|\mathrm{x})) = \sum_{\mathrm{i}=1}^{\mathrm{N}} -\ln\frac{1}{\sigma_\mathrm{i}} - \frac{(\mathrm{x_i} - \hat{\mathrm{x}}_\mathrm{i})^2}{2\sigma_\mathrm{i}^2} \qquad (1\text{–}1)$$

where Θ_k is the k^{th} vector of parameter values, $\mathrm{x_i}$ is the i^{th} observation from a vector of N observations, $\hat{\mathrm{x}}_\mathrm{i}$ is the model predicted value using Θ_k that corresponds to $\mathrm{x_i}$, σ_i is the standard deviation of the sample for $\mathrm{x_i}$. Because the actual values for σ_i were not available for either of the data sets used in this study, each σ_i was set to 5% of $\mathrm{x_i}$.

Within each iteration of the optimization, candidate values for each parameter were generated using a normal random walk routine. For each parameter, a step was sampled from a normal distribution with a mean of 0 and a standard deviation defined for each parameter ($\sigma_\mathrm{p}^{\mathrm{step}}$). The step was then added to the current value for the parameter (Θ_p) to produce the candidate value (Θ_p^*) subject to the maximum ($\Theta_\mathrm{p}^{\mathrm{max}}$) and minimum ($\Theta_\mathrm{p}^{\mathrm{min}}$) values defined for that parameter. Once candidate values were generated, the log-likelihood for the new value of each parameter was calculated by running CROPGRO with Θ_p^* and using the new model predictions as $\hat{\mathrm{x}}_\mathrm{i}$ in Eq. 1–1. An acceptance/rejection ratio (α) was then calculated by dividing the candidate likelihood ($\mathrm{L}(\Theta_\mathrm{p}^*|\mathrm{x})$, transformed back from the log-likelihood) by the likelihood of the previously

accepted parameter value ($\mathrm{L}(\Theta_\mathrm{p}|\mathrm{x})$), with the ratio being restricted to a maximum value of 1. A number (u) was randomly sampled from a uniform distribution ranging from 0 to 1 and if α was greater than u then the candidate value was accepted. Otherwise, the candidate value was discarded and the then current value was stored for the next iteration. The process was repeated until the candidate value for each parameter was either accepted or rejected, at which point the iteration was complete.

This optimization algorithm was iterated 5000 times for each parameter group and the values of all accepted values for each parameter were stored. The accepted values from the first 500 iterations were discarded, and the remaining accepted values were used to calculate a mean and standard deviation for each parameter. Initial ($\Theta_\mathrm{p}^\mathrm{init}$), maximum ($\Theta_\mathrm{p}^\mathrm{max}$), minimum ($\Theta_\mathrm{p}^\mathrm{min}$), and step standard deviation ($\sigma_\mathrm{p}^\mathrm{step}$) values for each parameter are given in Table 1-6 and 1-8. Literature sources for $\Theta_\mathrm{p}^\mathrm{init}$, $\Theta_\mathrm{p}^\mathrm{max}$, and $\Theta_\mathrm{p}^\mathrm{min}$ are also provided. Where no literature values were available, CROPGRO parameter values for other species were used to define the range and initial values. In the case of several parameters the values were conditional to the values of other parameters and, thus, no value $\Theta_\mathrm{p}^\mathrm{init}$, $\Theta_\mathrm{p}^\mathrm{max}$, or $\Theta_\mathrm{p}^\mathrm{min}$ is given. This is true of the tissue carbohydrate concentration parameters (PCARLF, PCARST, PCARSH, PCARSD) whose values were set as the difference between all other tissue composition parameters of the same type and 1. For example, the calculation for PCARLF would be:

$$\mathrm{PCARLF} = 1 - \mathrm{PLIPLF} - \mathrm{PLIGLF} - \mathrm{POALF} - \mathrm{PMINLF} - \mathrm{PROLFI}$$

where PLIPLF, PLIGLF, POALF, PMINLF, and PROLFI are parameters defined in Tables 1-3 and 1-5. Similarly, values for YSTEM(1-8) were set as follows:

$$\mathrm{YSTEM} = 1 - \mathrm{YROOT} - \mathrm{YLEAF}$$

where YSTEM is a vector of all YSTEM(1-8) values, YLEAF is a vector of YLEAF(1-8) values, and YROOT is a vector of YROOT(1-8) root partitioning values. Likewise,

FRSTMF was set as the difference between 1, FRRTF and FRLFF, where FRRTF is the final root partitioning during reproductive growth. The root partitioning values were set from observed data Maliro (1987). SDPROS, and SDPROG were set to the same value as SDPRO because parameter optimization was for the reference cultivar, in this case *76W*. YSLATM(2) and YSLATM(3) were set equal to YSLATM(1) because these parameters are generally set equal to each other.

1.3 Results and Discussion

1.3.1 Phenology

Results of the parameter optimization are shown in Tables 1-9 and 1-10. In general, the results show a high degree of certainty (i.e. low $\sigma_{\mathrm{p}}^{\mathrm{post}}$) with respect to the posterior means. Some of this may be an artifact of the limited data with which optimization was completed. Nevertheless, it is reasonable to conclude that the posterior means are good parameter estimates given the data used and the conditions defined in Tables 1-6 and 1-8. The phenology parameter values indicate a crop duration, under optimal temperature and daylength, of 108 days for *76W*, which corresponds well to that observed for *Prabhat*, an extra-short duration cultivar and parent to *76W*. Similarly, the duration for *ICPL 88039* under optimal conditions was 112 days, consistent with its classification as an extra-short duration cultivar at ICRISAT headquarters (17.5°N, 78.3°E) near Hyderabad, Andhrah Pradesh (Pande et al., 2006). The PPSEN value of 0.74 indicates sensitivity to photoperiod, confirming results by Chauhan et al. (2002). This finding explains the longer duration for the cultivar (180-200 days) when grown at Indore (V.S. Bhatia, personal communication, May 8, 2012). The FL-SD for *ICPL 88039* was long compared to the FL-SH value for the same cultivar (Table 1-10). Similarly, the values for R7-R8 and SFDUR were both unusually long when compared to the value for SD-PM. The issue with FL-SD, R7-R8, and SFDUR may be due to inaccuracies in the phenological data on which they were optimized.

1.3.2 Dry Matter – Gainesville, FL

Shoot mass predictions for the irrigated and rainfed treatments are shown in Figures 1-1A and 1-1B. As might be expected, the predictions for the calibration dataset (irrigated; Fig. 1-1A) are slightly better than for the validation dataset (rainfed; Fig. 1-1B). In general, the irrigated treatment did not show model bias, whereas the model consistently under-predicted shoot mass for the rainfed treatment. Nevertheless, both treatments showed high D and C_{eff} values with low RRMSE. Similar model performance was observed for leaf and stem mass, with D and C_{eff} values close to 1 (Fig. 1-2A, 1-2B, 1-3A, and 1-3B). Still, as observed for shoot mass, the model under-predicted leaf and stem mass for the rainfed treatment. The abrupt leveling-off of leaf and stem mass after flowering is captured well by the high value for XFRT (0.99) and is consistent with the characterization of *76W* as a determinate cultivar (Brakke, 1984). Pod and grain mass were both predicted remarkably well for the irrigated treatment (Fig. 1-4A and 1-5A).NA NA Rainfed pod mass and grain mass were predicted somewhat less well with C_{eff} values between 0.74 and 0.81. However, these lower values may be due to higher variability in the underlying data rather than problems in the model.

Differences in model predictions between irrigated and rainfed treatments were larger than observed with rainfed predictions NA NA for stem. In contrast, treatment differences in observed data were only 3% for leaf and less than 0% for stem. Treatment effects on pod and grain mass were less pronounced in model simulations than in observed data (Fig. 1-4A, 1-4B, 1-5A, and 1-5B). Observed final pod and grain mass were reduced by 44% and 49%, whereas simulated final pod and grain mass were reduced by only % and %. Plots of simulated water stress (scaled between 0 and 1) showed a peak of 0.68 at approximately 90 DAP and tapering off to 0 by 100 DAP (data not shown). This fits observations that the most severe drought stress occurred between 80 and 100 DAP. The reduction in simulated growth within this period demonstrates that the model is capturing this effect (Fig. 1-1B).

1.3.3 Leaf Area – Gainesville, FL

Leaf area index (LAI) was also predicted fairly well, but the time series and 1:1 plots both indicate a tendency for under-prediction of LAI during peak vegetative growth and slight over-prediction late in the season for the irrigated treatment (Fig. 1-6A). The under-prediction is largely a function of low specific leaf area (SLA) predictions, particularly after flowering occurred at about 70 days after planting (DAP) (Fig. 1-7A). The problem with SLA predictions appears to be an issue with model structure, possibly due to the handling of secondary thickening and leaf senescence at the canopy level rather than leaf level. Nevertheless, model simulations of SLA show a similar time trend as that in the observed data, namely, increasing during primary leaf area expansion and subsequently decreasing during reproductive growth. The model captured the rainfed LAI dynamics well, despite under-predicting SLA between 60 and 80 DAP (Fig. 1-6B and 1-7B). It appears that the under-prediction of SLA coincided with an over-prediction in leaf mass (Fig. 1-2B) resulting in an accurate prediction of LAI.

1.3.4 Nitrogen Concentration – Gainesville, FL

Results for prediction of leaf and stem N concentration dynamics were mixed. The overall trend of model predictions matches that of the data ($D > 0.77$, Fig. 1-8A, 1-8B, 1-9A, and 1-9B). However, the substantially lower values for C_{eff} indicate that prediction of the data is still fairly poor. Shell N concentration was predicted better with $D = 0.93$ and $C_{eff} = 0.77$. Grain N concentration predictions were better than the D and C_{eff} statistics indicate, especially given that, on average, predictions were within 0.03 of observed values (Fig. 1-11). The low D and C_{eff} values are a result of very little variation in the observed grain N concentration rather than poor prediction by CROPGRO. The causes for the leaf and stem N dynamics may relate to the issue with SLA prediction discussed above (i.e. the simulation of N dynamics at the whole canopy level rather than at leaf level). Treatment effects on N concentration were small in both observed and predicted data.

1.3.5 Dry Matter – Indore, India

Shoot mass for the Indore, India data set was predicted well with a D value of 0.98 and C_{eff} of 0.93 (Fig. 1-12A). Nevertheless, the under-prediction of shoot mass late in the season is noticeable, a phenomenon mirrored in predictions of grain mass (Fig. 1-12B). Good predictions of harvest index indicate that partitioning between vegetative and reproductive tissues are simulated well (Fig. 1-13) The under-prediction appears to be a result of simulated water stress after 195 DAP, reducing total dry matter production and thereby both shoot and grain mass. Given that 195 DAP is approximately 2 months into the dry season for Indore, it would not be surprising to see water stress. However, observed data did not indicate water stress given that shoot and grain mass continued increasing until final harvest (Fig. 1-12A and 1-12B). This discrepancy may be due to inaccuracies in soil water input data. Gijsman et al. (2002) found that estimating accurate values of volumetric water content for soil lower limit (SLLL), drained upper limit (SDUL), and saturated (SSAT) conditions was difficult and could have substantial impact on subsequent model simulations. It should be noted here that the SLLL values originally estimated using soil texture were lowered based on time-series volumetric soil water content measurements (data not shown). In addition, SRGF had to be increased to 1.0 for all soil layers (Table 1-2) to achieve levels of soil water extraction by roots that were adequate to match the dynamics observed in the soil water data. Despite these adjustments, the above-mentioned NA late in the season.

Figure 1-14A shows shoot mass for *76W* and *ICPL 88039* simulated at Gainesville in 1984 and Indore in 2003. *76W* produced more dry matter than *ICPL 88039* in both locations. The difference in dry matter production is a function of higher LFMAX value for *76W* (Tables 1-9 and 1-10) and higher simulated SLA for *ICPL 88039* (data not shown). The effect of SLA (or its reciprocal specific leaf weight; SLW) on photosynthetic rate is controlled by the species parameter SLWREF, whose value of 0.0035 g $cm^{-2}$was kept from soybean. Instantaneous photosynthetic rate is scaled higher if SLW is high

(SLA is low) and lower if SLW is low (SLA is high). Thus, the higher LFMAX and lower SLA values in *76W* resulted in higher photosynthetic rates and correspondingly higher dry matter accumulation than *ICPL 88039*. The reason for higher SLA in *ICPL 88039* relates to its slower development rate, which is caused by its short critical photoperiod (CSDL = 11.60) and sensitivity to photoperiod (PPSEN = 0.74). Currently, CROPGRO simulates leaf secondary thickening by reducing the SLA of new leaf tissue as crop development progresses. Thus, when crop development is slowed, as in the present case, SLA reduction also slows. Slow crop development is also the cause of the lack of grain growth for *ICPL 88039* at Gainesville (Fig. 1-15A). Model outputs show that *ICPL 88039* only reached stage R3 (beginning pod growth) just before the end of simulation (due to a freeze event). A similar phenomenon was noted by Chauhan et al. (2002), where the authors observed that *ICPL 88039* produced virtually no grain mass by harvest time when grown in Suwon, Korea (37.3°N, 127.0°W). Simulated grain mass for *ICPL 88039* at Indore was better, although approximately half of simulated grain mass for *76W* (Fig. 1-15B). Interestingly, *76W* achieved maturity in both locations and simulated grain mass was fairly consistent across locations (around 3000 kg ha^{-1}).

1.3.6 Parameter Optimization

In general, the parameter optimization algorithm worked well at estimating realistic values for parameters with good correspondence to observed data. One major challenge in the process was overcoming the lack of σ_i for observed data. Setting σ_i to a set percentage of x_i fits general trends in measurement variances of growth analysis data, which tend to increase with larger measurements at later sampling dates. However, such an approach creates an implicit weighting of observations of smaller magnitude, an effect that is especially pronounced in situations where some data are orders of magnitude different than others. Ideally, σ_i should be derived from actual measurements and thereby genuinely reflect the uncertainty of x_i with respect to other measurements. Nevertheless, as the present study shows, reasonable results can be

achieved even when approximations of σ_i are used, a finding that is particularly relevant for use of this algorithm with historic datasets comprised of only observation means.

Another challenge was the choice of data to use when estimating phenology parameters. Initially, optimization of phenology parameters was done using only phenology data. Though the results matched observed phenology, the optimized values of the phenology parameters prevented accurate simulation of dry matter dynamics. The sequential nature of the parameter optimization approach used in this study accentuated this effect by preventing good estimates of subsequent parameters. There are two possible contributors to this phenomenon. The first is inadequate formulation of the linkages between phenological events and reproductive growth dynamics in the model. The second contributor is inaccurate phenology data. Day of first pod and day of first seed can be especially difficult to determine accurately depending on the sampling interval, sample size, and uniformity of the stand, among other factors. Thus, when available, it seems preferable to use early pod and seed mass to estimate these parameters (FL-SH and FL-SD) as was done for the final parameter estimation with the Gainesville, FL 1984 data set (Table 1-6).

1.3.7 Summary and Conclusions

Overall, the results of this study show that CROPGRO can be used to simulate the growth and development of pigeonpea. However, revision of N concentration parameters or possible reformulation of model code handling N concentration dynamics may be needed to better predict these dynamics. Likewise, better formulation of model code is likely needed in order to improve predictions of phenological events and the subsequent pod and seed growth. In addition, further testing of CROPGRO with other data sets is needed to confirm the accuracy of all the parameter estimates developed from this study. For example, datasets from serial sowing date or multi-location trials would assure greater accuracy in estimating CSDL and PPSEN values. Nevertheless, based

on the results of this study, CROPGRO can be used to reliably predict pigeonpea growth and development under diverse environmental conditions.

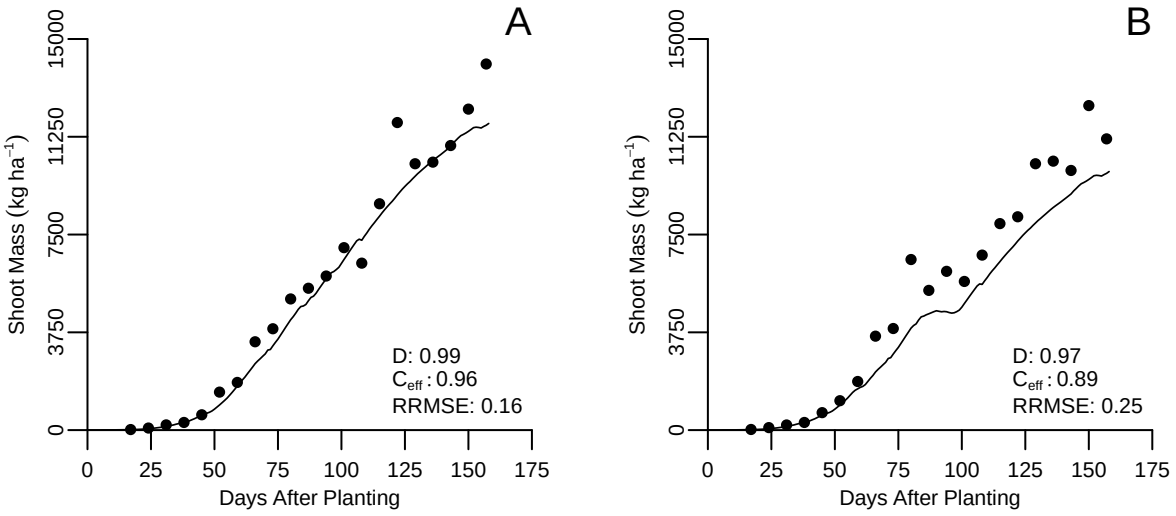

Figure 1-1. Time series of observed and predicted shoot mass for irrigated (A) and rainfed (B) pigeonpea grown near Gainesville, FL in 1984.

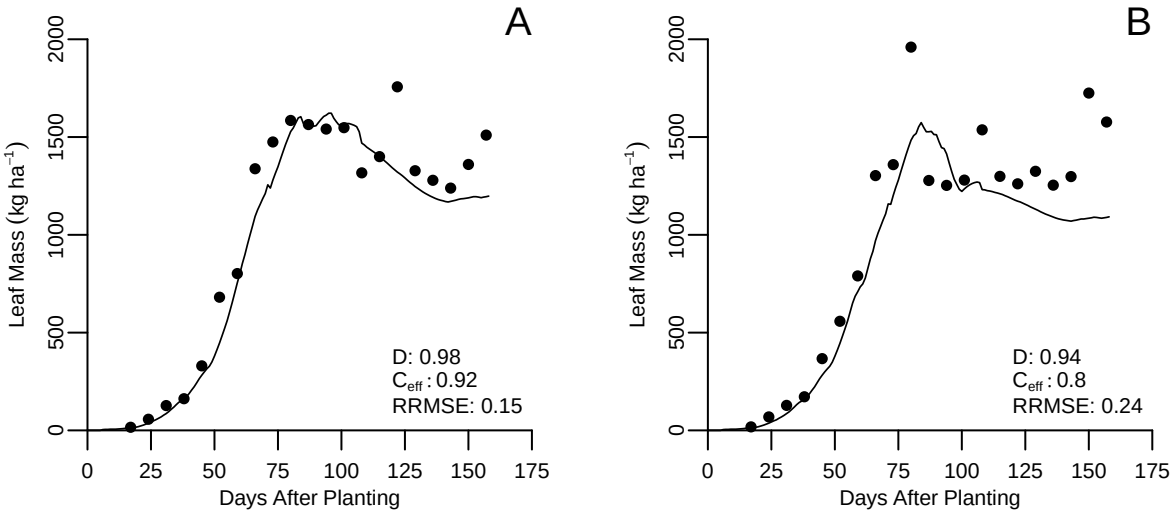

Figure 1-2. Time series of observed and predicted leaf mass for irrigated (A) and rainfed (B) pigeonpea grown near Gainesville, FL in 1984.

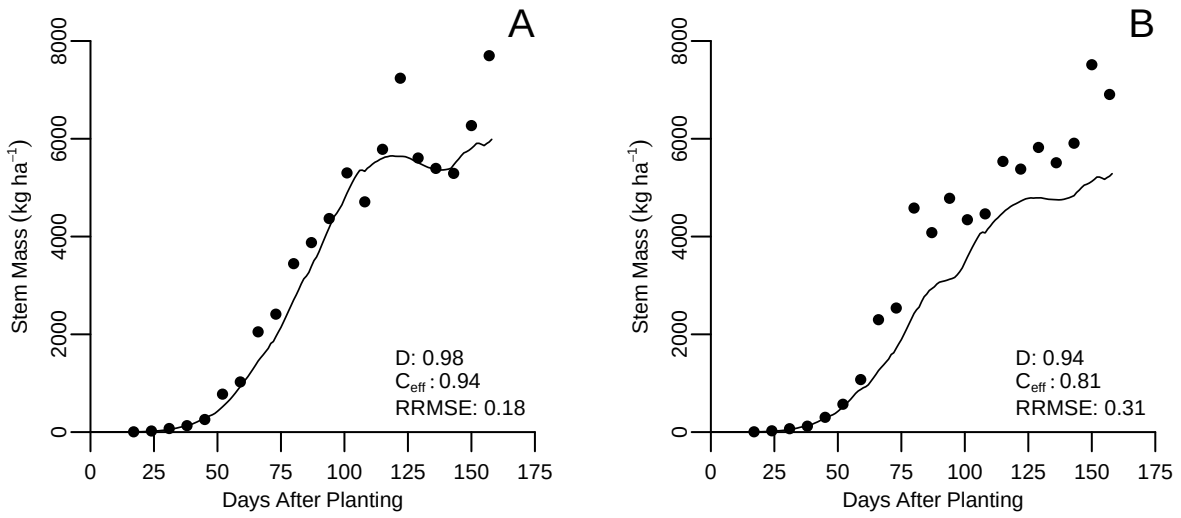

Figure 1-3. Time series of observed and predicted stem mass for irrigated (A) and rainfed (B) pigeonpea grown near Gainesville, FL in 1984.

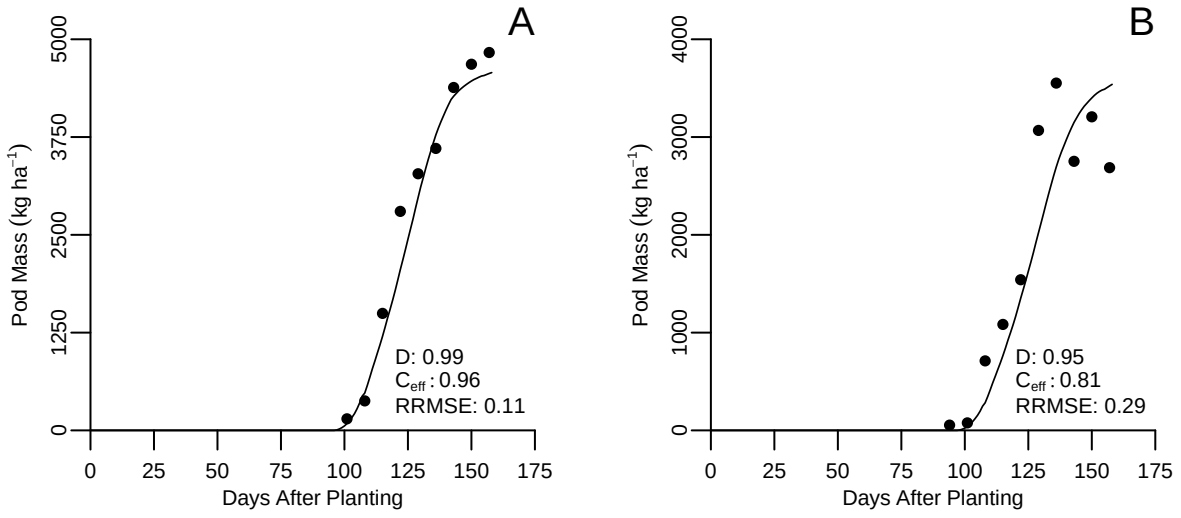

Figure 1-4. Time series of observed and predicted pod mass for irrigated (A) and rainfed (B) pigeonpea grown near Gainesville, FL in 1984.

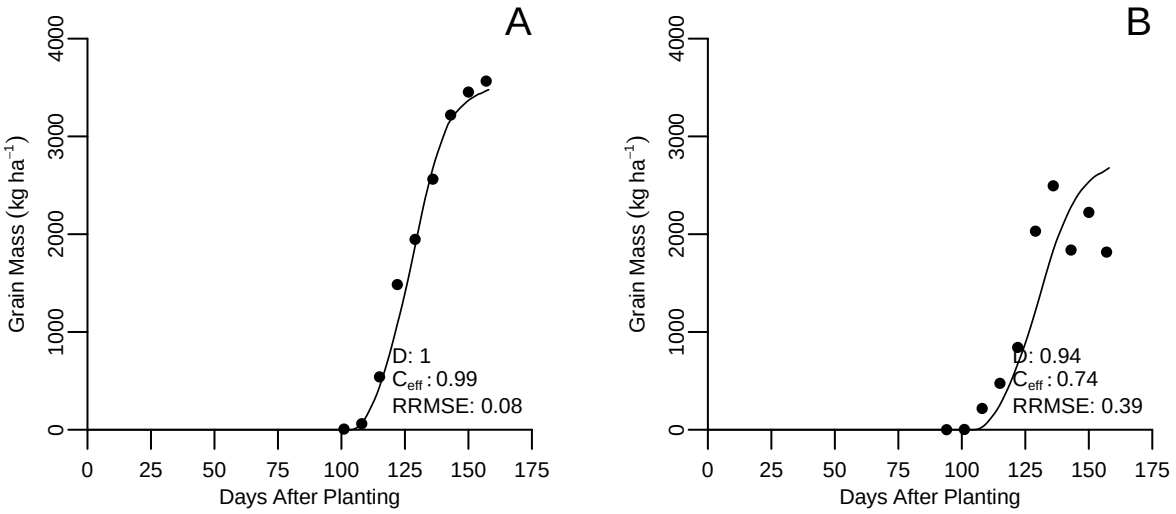

Figure 1-5. Time series of observed and predicted grain mass for irrigated (A) and rainfed (B) pigeonpea grown near Gainesville, FL in 1984.

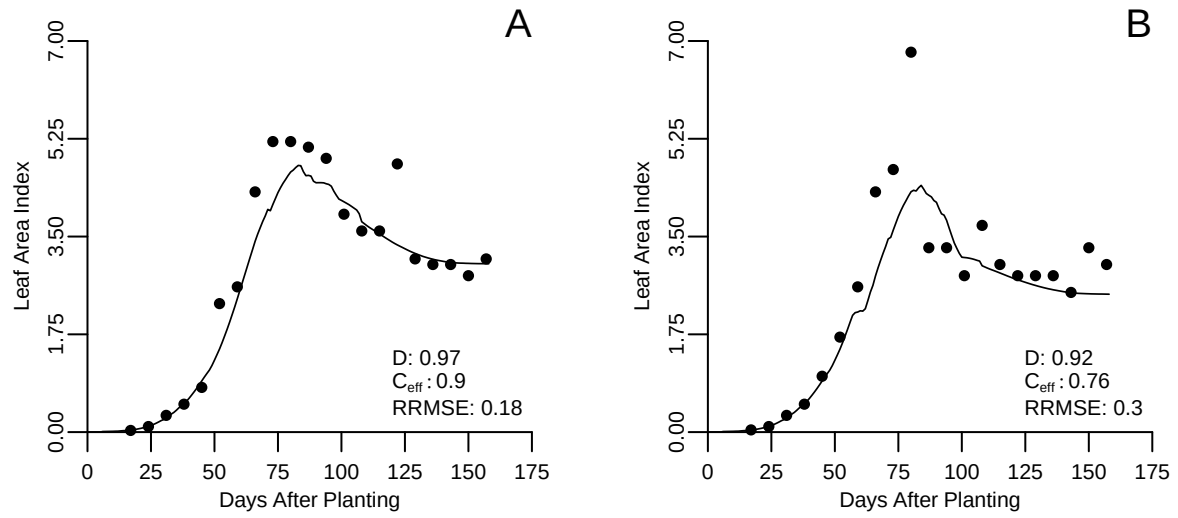

Figure 1-6. Time series of observed and predicted leaf area index for irrigated (A) and rainfed (B) pigeonpea grown near Gainesville, FL in 1984.

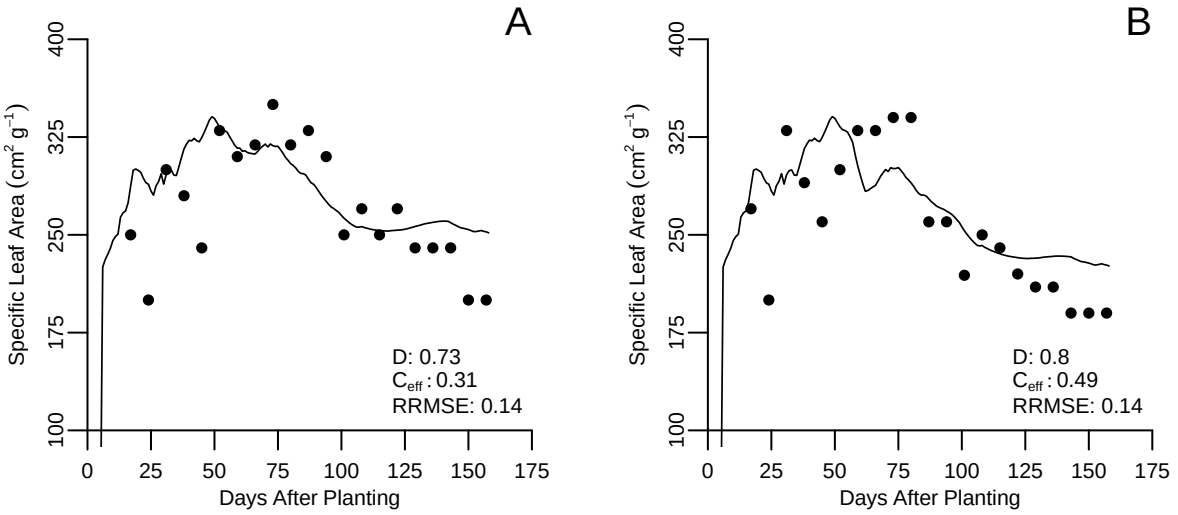

Figure 1-7. Time series of observed and predicted specific leaf area for irrigated (A) and rainfed (B) pigeonpea grown near Gainesville, FL in 1984.

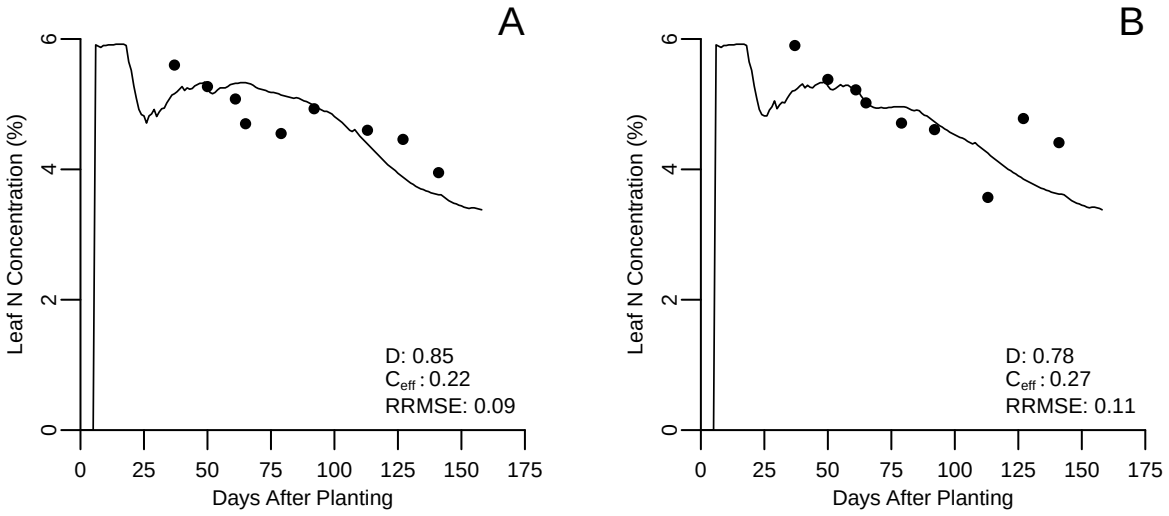

Figure 1-8. Time series of observed and predicted leaf N concentration for irrigated (A) and rainfed (B) pigeonpea grown near Gainesville, FL in 1984.

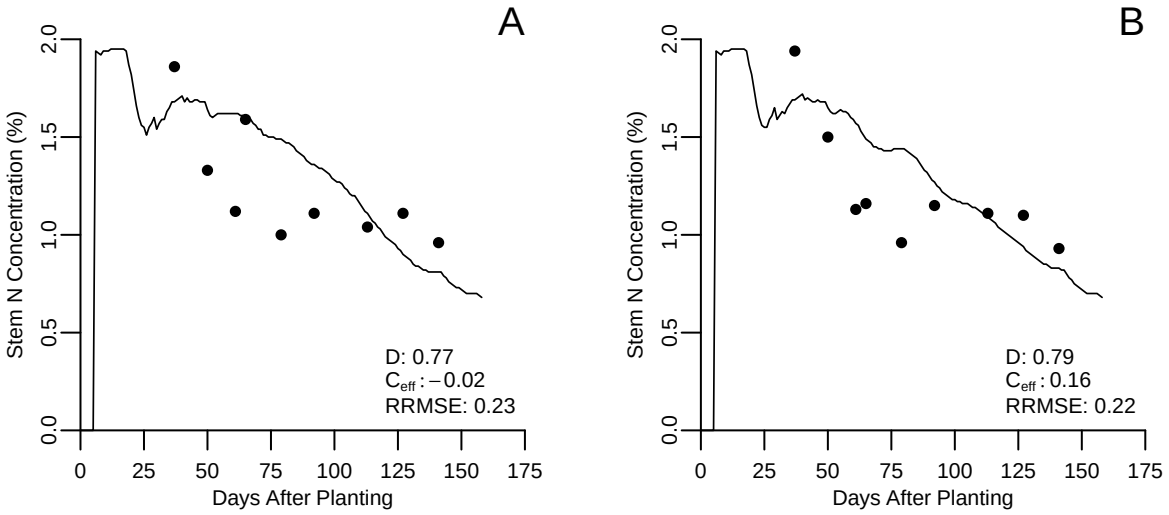

Figure 1-9. Time series of observed and predicted stem N concentration for irrigated (A) and rainfed (B) pigeonpea grown near Gainesville, FL in 1984.

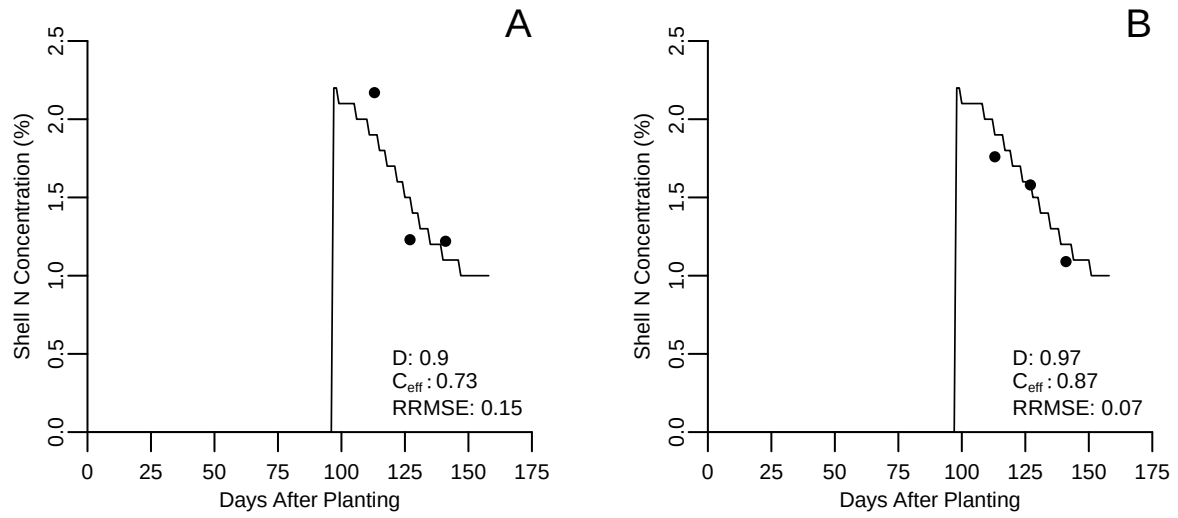

Figure 1-10. Time series of observed and predicted shell N concentration for irrigated (A) and rainfed (B) pigeonpea grown near Gainesville, FL in 1984.

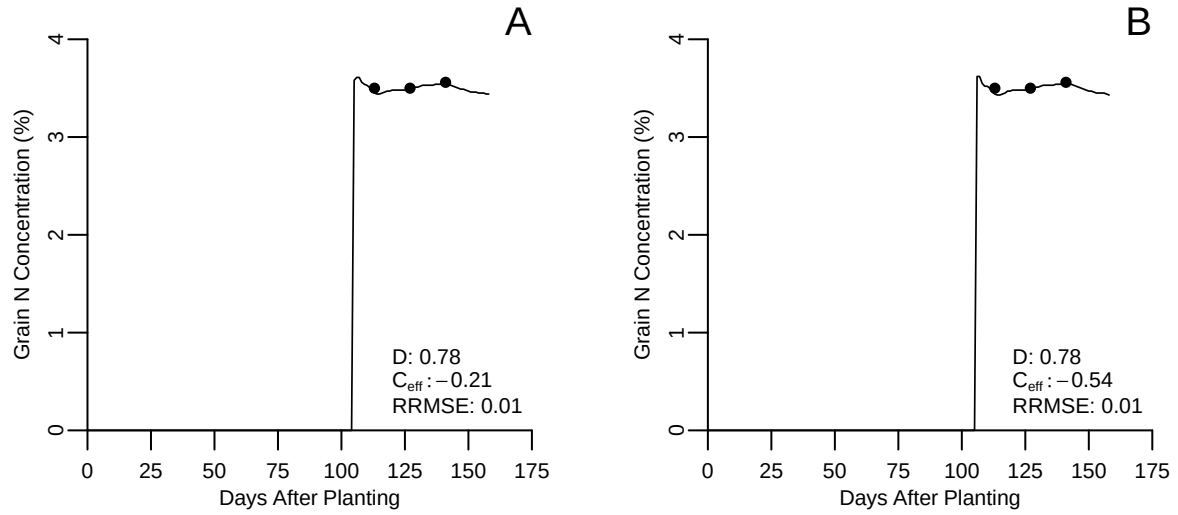

Figure 1-11. Time series of observed and predicted grain N concentration for irrigated (A) and rainfed (B) pigeonpea grown near Gainesville, FL in 1984.

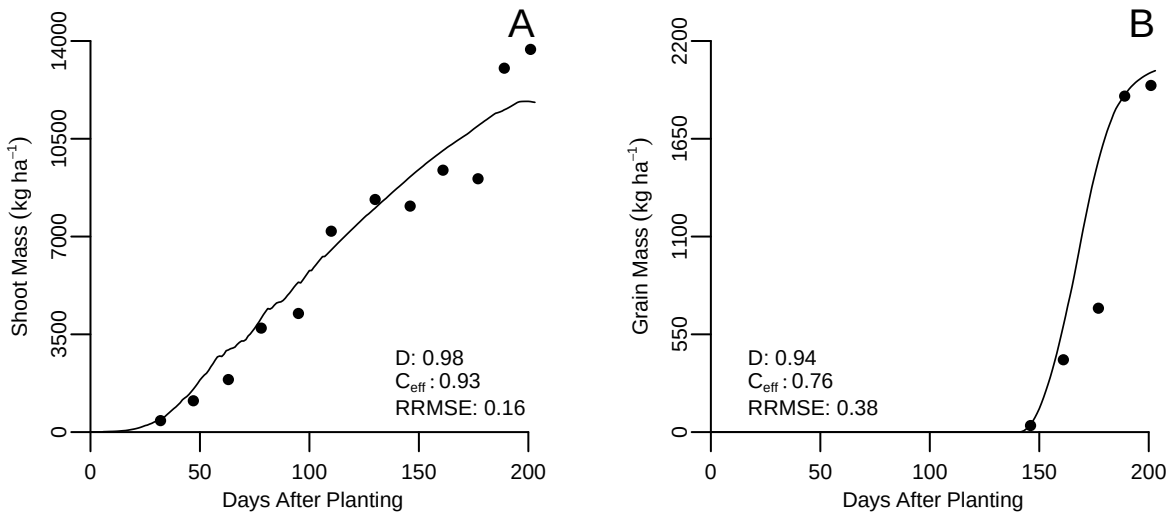

Figure 1-12. Time series of observed and predicted shoot mass for rainfed pigeonpea grown near Indore, Madhya Pradesh, India in 2003.

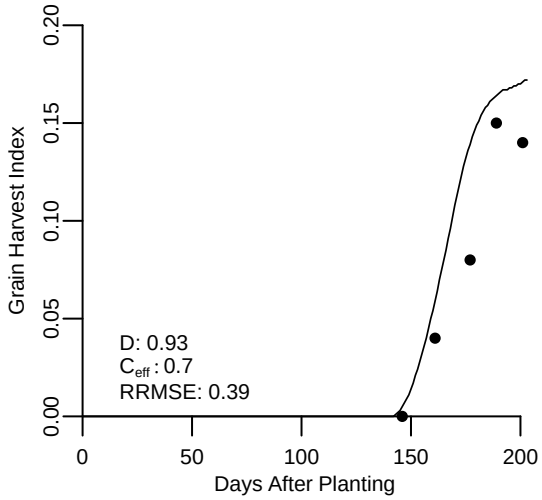

Figure 1-13. Time series of observed and predicted grain harvest index for rainfed pigeonpea grown near Indore, Madhya Pradesh, India in 2003.

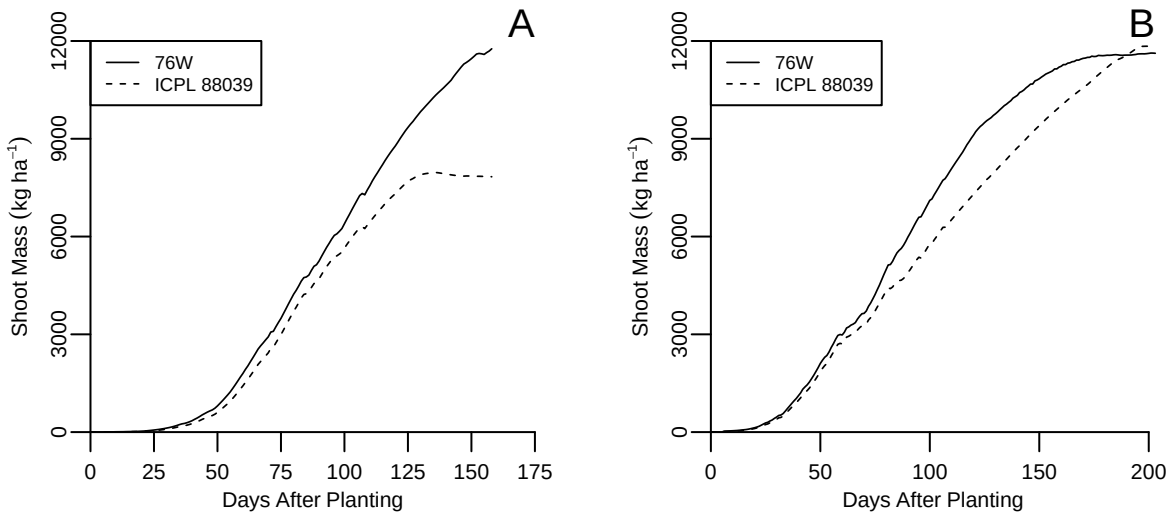

Figure 1-14. Shoot mass for two cultivars as simulated at Gainesville, FL in 1984 (A) and Indore, Madhya Pradesh, India in 2003 (B).

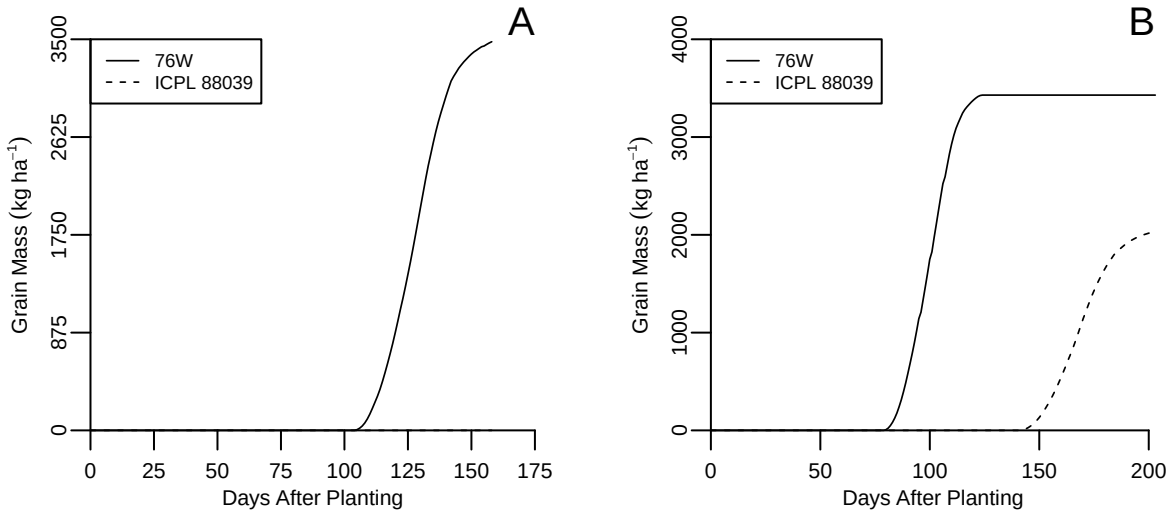

Figure 1-15. Grain mass for two cultivars as simulated at Gainesville, FL in 1984 (A) and Indore, Madhya Pradesh, India in 2003 (B).

Table 1-1. Soil profile characteristics for a Kendrick Fine Sand (Loamy, siliceous, semiactive, hyperthermic Arenic Paleudults) near Gainesville, FL as used to simulate pigeonpea growth with the CSM-CROPGRO model.

SLB	SLLL	SDUL	SSAT	SRGF	SSKS	SBDM	SLOC	SH_2O	SNH_4	SNO_3	SOM_1	SOM_2	SOM_3
5	0.02	0.09	0.23	1.00	7.40	1.36	0.90	0.09	1.50	0.60	0.00	0.02	0.98
15	0.02	0.09	0.23	1.00	7.40	1.40	0.69	0.09	1.50	0.60	0.00	0.02	0.98
30	0.02	0.09	0.23	0.50	15.80	1.46	0.28	0.09	1.50	0.60	0.00	0.02	0.98
45	0.02	0.09	0.23	0.29	28.00	1.47	0.20	0.09	1.50	0.60	0.00	0.02	0.98
60	0.02	0.09	0.23	0.29	28.00	1.47	0.20	0.09	1.50	0.60	0.00	0.02	0.98
90	0.02	0.08	0.23	0.38	27.60	1.43	0.09	0.08	0.60	0.60	0.00	0.02	0.98
120	0.02	0.08	0.23	0.07	17.50	1.48	0.03	0.08	0.50	0.60	0.00	0.02	0.98
150	0.03	0.13	0.23	0.03	0.30	1.57	0.03	0.13	0.50	0.60	0.00	0.02	0.98
180	0.07	0.26	0.36	0.01	0.10	1.79	0.03	0.26	0.50	0.60	0.00	0.02	0.98

SLB, depth to base of soil layer (cm); SLLL, soil lower limit (cm^3 cm^{-3}); SDUL, soil drained upper limit (cm^3 cm^{-3}); SSAT, soil saturated upper limit (cm^3 cm^{-3}); SBDM, soil bulk density, moist (g cm^{-3}); SLOC, soil organic carbon (%); SH_2O, Initial soil water content, (cm^3 cm^{-3}); SNH_4, Initial ammonium, (g elemental N Mg^{-1} soil); SNO_3, Initial soil nitrate, (g elemental N Mg^{-1} soil); SOM_1, Initial microbial soil organic matter (SOM) fractional composition (unitless); SOM_2, Initial intermediate SOM fractional composition (unitless); SOM_3, Initial passive SOM fractional composition (unitless); SOM_1+SOM_2+SOM_3 = 1.0.

Table 1-2. Soil profile characteristics for a Black Soil (Fine, Montmorillonitic Typic Haplustert) near Indore, Madhya Pradesh, India as used to simulate pigeonpea growth with the CSM-CROPGRO model.

SLB	SLLL	SDUL	SSAT	SRGF	SBDM	SLOC	SH_2O	SNH_4	SNO_3	SOM_1	SOM_2	SOM_3
5	0.18	0.40	0.60	1.00	1.36	0.60	0.27	0.01	0.01	0.00	0.02	0.98
15	0.18	0.40	0.60	1.00	1.36	0.60	0.27	0.01	0.01	0.00	0.02	0.98
30	0.18	0.40	0.60	1.00	1.36	0.60	0.27	0.01	0.01	0.00	0.02	0.98
45	0.18	0.39	0.60	1.00	1.36	0.64	0.21	0.01	0.01	0.00	0.02	0.98
60	0.18	0.39	0.60	1.00	1.36	0.64	0.21	0.01	0.01	0.00	0.02	0.98
90	0.18	0.39	0.60	1.00	1.36	0.64	0.17	0.01	0.01	0.00	0.02	0.98
120	0.18	0.39	0.60	1.00	1.36	0.60	0.39	0.01	0.01	0.00	0.02	0.98
150	0.18	0.39	0.60	1.00	1.36	0.60	0.39	0.01	0.01	0.00	0.02	0.98
160	0.18	0.39	0.60	1.00	1.36	0.60	0.39	0.01	0.01	0.00	0.02	0.98

See Table 1-1 for parameter definitions.

Table 1-3. Description of CROPGRO parameters modified for pigeonpea directly from literature.

Parameter	Type	Units	Description
PLIPLF	Species	fraction	Lipid fraction of leaf tissue
PLIPSD	Species	fraction	Lipid fraction of seed tissue
PLIPSH	Species	fraction	Lipid fraction of pod shell tissue
PLIPST	Species	fraction	Lipid fraction of stem tissue
PLIGLF	Species	fraction	Lignin fraction of leaf tissue
PLIGSD	Species	fraction	Lignin fraction of seed tissue
PLIGSH	Species	fraction	Lignin fraction of pod shell tissue
PLIGST	Species	fraction	Lignin fraction of stem tissue
PMINLF	Species	fraction	Mineral fraction of leaf tissue
PMINSD	Species	fraction	Mineral fraction of seed tissue
PMINSH	Species	fraction	Mineral fraction of pod shell tissue
PMINST	Species	fraction	Mineral fraction of stem tissue
POALF	Species	fraction	Organic acid fraction of leaf tissue
POAST	Species	fraction	Organic acid fraction of stem tissue
POASH	Species	fraction	Organic acid fraction of pod shell tissue
POASD	Species	fraction	Organic acid fraction of seed tissue
$T_{b,early}$	Species	°C	Base temperature for early reproductive growth
$T_{b,veg}$	Species	°C	Base temperature for vegetative growth
$T_{opt1,early}$	Species	°C	First optimum temperature for early reproductive growth
$T_{opt2,early}$	Species	°C	Second optimum temperature for early reproductive growth
$T_{opt1,late}$	Species	°C	First optimum temperature for late reproductive growth
XVGROW(1-6)	Species	node number	Vegetative stage values for YVREF(1-6)
YVREF(1-6)	Species	cm^2 $plant^{-1}$	Maximum leaf area at corresponding vegetative stage in XVGROW(1-6)

Table 1-4. Parameter names, values and literature sources for parameter values set based on the scientific literature. Parameters without literature source listed were set based on Maliro (1987).

Parameter	Value	Source
XVGROW(1-6)	0.0, 2.0, 4.0, 6.0, 8.0, 10.0	
YVREF(1-6)	1.0, 33.0, 55.0, 87.0, 124.0, 152.0	
PLIPLF	0.025	
PLIPST	0.020	
PLIPSH	0.020	
PLIPSD	0.015	
PLIGLF	0.070	
PLIGST	0.180	
PLIGSH	0.070	
PLIGSD	0.030	
POALF	0.050	
POAST	0.050	
POASH	0.050	
POASD	0.050	
PMINLF	0.094	
PMINST	0.046	
PMINSH	0.079	
PMINSD	0.048	
$T_{b,veg}$	10.0	Ranganathan et al. (2001)
$T_{b,early}$	10.0	Carberry et al. (2001)
$T_{opt1,early}$	20.0	Carberry et al. (2001)
$T_{opt2,early}$	24.0	Carberry et al. (2001)
$T_{opt1,late}$	26.0	Carberry et al. (2001)

Table 1-5. Description of CROPGRO species, ecotype, and cultivar parameters modified for pigeonpea using parameter optimization

Parameter	Type	Units	Description
CSDL	Cultivar	h	Critical short day length below which reproductive development progresses with no daylength effect (for shortday plants) (hour)
EM-FL	Cultivar	PD†	Time between plant emergence and flower appearance (R1)
FL-LF	Cultivar	PD	Time between first flower (R1) and end of leaf expansion
FL-SD	Cultivar	PD	Time between first flower and first seed (R5)
FL-SH	Cultivar	PD	Time between first flower and first pod (R3)
FL-VS	Ecotype	PD	Time from first flower to last leaf on main stem
FRLFF	Species	fraction	Daily dry matter partitioning to leaf after end of leaf expansion
FRSTMF	Species	fraction	Daily dry matter partitioning to stem after end of leaf expansion
ICMP	Species	mol photon $m^{-2}d^{-1}$	Photosynthetically active radiation compensation point below which leaf senescence occurs
LFMAX	Cultivar	mg CO_2 $m^{-2}s^{-1}$	Maximum leaf photosynthesis rate at 30°C, 350 ppm CO_2, and high light
NMOBMX	Species	fraction d^{-1}	Maximum N mobilization rate during late reproductive growth (beyond R5)
NVSMOB	Species	fraction	Fraction of NMOBMX used during vegetative growth
PCARLF	Species	fraction	Carbohydrate concentration of leaf
PCARSD	Species	fraction	Carbohydrate concentration of seed
PCARSH	Species	fraction	Carbohydrate concentration of shell
PCARST	Species	fraction	Carbohydrate concentration of stem
PL-EM	Cultivar	°C-d	Time between planting and emergence (V0)
PORPT	Species	g petiole g^{-1} leaf	ratio of petiole mass to leaf mass
PPSEN	Cultivar	h^{-1}	Relative response of development to photoperiod with time
PROLFF	Species	fraction	Final leaf protein concentration
PROLFG	Species	fraction	Leaf protein concentration for normal growth
PROLFI	Species	fraction	Maximum leaf protein concentration
PROSHF	Species	fraction	Final shell protein concentration
PROSHG	Species	fraction	Shell protein concentration for normal growth

Table 1-5. (continued)

Parameter	Type	Units	Description
PROSHI	Species	fraction	Maximum shell protein concentration
PROSTF	Species	fraction	Final stem protein concentration
PROSTG	Species	fraction	Stem protein concentration for normal growth
PROSTI	Species	fraction	Maximum stem protein concentration
R1PPO	Cultivar	h	Increase in daylength sensitivity after R1
R7-R8	Cultivar	d	Time between physiological (R7) and harvest maturity (R8)
SD-PM	Cultivar	PD	Time between first seed (R5) and physiological maturity (R7)
SDPDV	Cultivar	seed number pod^{-1}	Average seed per pod under standard growing conditions
SDPRO	Species	fraction	Cultivar standard seed protein concentration
SDPROG	Species	fraction	Normal growth seed protein concentration for reference cultivar
SDPROS	Species	fraction	Standard seed protein concentration for reference cultivar
SENRTE	Species	g leaf g^{-1} protein	Amount of leaf senescence due to protein mobilization (after exhausting available leaf protein)
SFDUR	Cultivar	PD	Seed filling duration for pods at standard growth conditions
SLAMAX	Species	cm^2 g^{-1}	Maximum specific leaf area grown under low light
SLAMIN	Species	cm^2 g^{-1}	Minimum specific leaf area grown under high light
THRSH	Cultivar	g seed g^{-1} pod	Threshing percentage, maximum ratio of seed mass to pod mass at maturity
TRIFL	Ecotype	leaves °C-d^{-1}	Rate of leaf appearance on the mainstem
WTPSD	Cultivar	g $seed^{-1}$	Maximum mass per seed
XFRT	Cultivar	fraction	Maximum fraction of daily growth that is partitioned to seed and shell
XLEAF(1-8)	Species	node number	Vegetative stage values for YLEAF(1-8) and YSTEM(1-8)
XSLATM(1-5)	Species	°C	Temperatures corresponding to YSLATM(1-5)
YLEAF(1-8)	Species	fraction d^{-1}	Daily dry matter partitioning to leaf corresponding to XLEAF(1-8)
YSLATM(1-5)	Species	fraction	Relative temperature effect on specific leaf area of new leaves
YSTEM(1-8)	Species	fraction d^{-1}	Daily dry matter partitioning to stem corresponding to XLEAF(1-8)

†PD, photothermal days

Table 1-6. Grouping of parameters in order of optimization, minimum (Θ_p^{min}), maximum (Θ_p^{max}), initial (Θ_p^{init}), and step standard deviation (σ_p^{step}) values for parameters estimated based on optimization with Gainesville, FL 1984 dataset. Crop data used and literature sources are listed by parameter group. Crop data abbreviations are explained in Table 1-7.

Group	Parameter	Θ_p^{min}	Θ_p^{max}	Θ_p^{init}	σ_p^{step}	Crop data	Source
1	PL-EM	2.7	11.2	5.00	0.38	EDAP	Lawn and Troedson (1990); Ranganathan et al. (2001)
2	EM-FL	10.7	60.0	46.0	1.30	ADAP	Carberry et al. (2001);
	CSDL	11.00	14.00	12.5	0.05		Chauhan et al. (2002);
	PPSEN	0.12	1.00	0.25	0.014		Troedson et al. (1990)
3	FL-SH	2.5	22.0	18.0	1.00	$PWAD_{early}$	Robertson et al. (2001a,b)
	R1PPO	0.189	0.504	0.500	0.01		
4	FL-SD	2.5	30.0	28.0	1.00	$GWAD_{early}$	Robertson et al. (2001a)
5	SD-PM	22.7	40.0	36.0	2.50	MDAP	
6	R7-R8	7.0	21.0	14.0	0.7	R8AP	
7	PROLFI	0.298	0.372	0.340	0.006	LN%D, SN%D,	Devries et al. (1989b);
	PROLFG	0.230	0.298	0.266	0.004	SHND, GN%D	Sanetra et al. (1998)
	PCARLF			0.421			
	PROLFF	0.094	0.230	0.200	0.006		
	PROSTI	0.110	0.140	0.115	0.002		
	PROSTG	0.070	0.110	0.081	0.002		
	PCARST			0.589			
	PROSTF	0.050	0.070	0.058	0.002		
	PROSHI	0.122	0.182	0.172	0.004		
	PROSHG	0.095	0.143	0.126	0.002		

Table 1-6. (continued)

Group	Parameter	Θ_p^{min}	Θ_p^{max}	Θ_p^{init}	σ_p^{step}	Crop data	Source
	PCARSH			0.609			
	PROSHF	0.050	0.080	0.068	0.003		
	SDPROS	0.178	0.268	0.207	0.004		
	SDPROG			0.207			
	SDPRO			0.207			
	PCARSD			0.650			
	NMOBMX	0.065	0.148	0.068	0.004		
	NVSMOB	0.30	0.40	0.35	0.01		
8	TRIFL	0.36	0.88	0.76	0.020	L#SD	Ranganathan et al. (2001)
	FL-VS	9.0	29.0	19.35	1.0		
9	SLAMAX	590	990	900	2.5	SLAD	Lopez et al. (1997)
	SLAMIN	200	300	275	2.5		
	XSLATM(3)	9.8	12.2	11.0	0.1		
	XSLATM(4)	16.5	27.0	22.0	0.2		
	YSLATM(1)	0.20	0.30	0.25	0.05		
	YSLATM(2)			0.25			
	YSLATM(3)			0.25			
	FL-LF	15.0	32.0	25.53	1.0		
10	YLEAF(1)	0.45	0.55	0.50	0.02	$LFFD_{veg}$, $STFD_{veg}$,	
	YLEAF(2)	0.45	0.55	0.50	0.02	$RTFD_{veg}$	
	YLEAF(3)	0.45	0.55	0.50	0.02		
	YLEAF(4)	0.45	0.55	0.50	0.02		
	YLEAF(5)	0.35	0.45	0.40	0.02		
	YLEAF(6)	0.35	0.45	0.40	0.02		
	YLEAF(7)	0.25	0.35	0.30	0.02		
	YLEAF(8)	0.15	0.25	0.20	0.02		

Table 1-6. (continued)

Group	Parameter	Θ_p^{min}	Θ_p^{max}	Θ_p^{init}	σ_p^{step}	Crop data	Source
	YSTEM(1)			0.10			
	YSTEM(2)			0.15			
	YSTEM(3)			0.20			
	YSTEM(4)			0.25			
	YSTEM(5)			0.40			
	YSTEM(6)			0.40			
	YSTEM(7)			0.50			
	YSTEM(8)			0.60			
11	XFRT	0.60	1.00	0.80	0.015	HIPD	
12	FRLFF	0.05	0.25	0.11	0.02	$LFFD_{rep}$,	Sharma and Saxena (1983)
	FRSTMF			0.69		$STFD_{rep}$	
	SENRTE	0.50	1.00	0.80	0.03		
	ICMP	0.80	1.80	1.40	0.05		
	PORPT	0.10	0.15	0.13	0.01		
13	LFMAX	0.80	1.10	1.00	0.02	CWAD	Lopez et al. (1988)
14	SDPDV	1.6	4.0	3.5	0.10	G#PD	Remanandan (1990)
15	THRSH	5.3	90.0	74.0	3.0	$SH\%D_{harv}$	Remanandan (1990)
16	SFDUR	24.5	40.0	29.0	2.0	GWGD	Remanandan (1990)
	PODUR	4.0	24.0	20.0	0.6	SH%D	
	WTPSD	0.15	0.25	0.17	0.02		

Table 1-7. Definitions of crop data used for optimization

Data Abbreviation	Crop Data	Units
ADAP	Anthesis (R1) day	DAP†
CWAD	Shoot mass	kg ha^{-1}
CWAM	Shoot mass at maturity	kg ha^{-1}
EDAP	Emergence day	DAP
G#PD	Grain number per pod	grains pod^{-1}
GN%D	Grain N concentration	percent
GWAD	Grain mass	kg ha^{-1}
$GWAD_{early}$	Grain mass for first two weeks of grain growth	kg ha^{-1}
GWGD	Grain unit mass	g $grain^{-1}$
H#AM	Grain number at maturity	grains m^{-2}
HIPD	Pod harvest index	kg pod kg^{-1} shoot
HWAM	Grain mass at maturity	kg grain ha^{-1}
HWUM	Grain unit mass at maturity	g $grain^{-1}$
L#SD	Main stem node number	nodes $plant^{-1}$
$LFFD_{rep}$	Fraction leaf during reproductive growth	kg leaf kg^{-1} shoot
$LFFD_{veg}$	Fraction leaf during vegetative growth	kg leaf kg^{-1} shoot
LN%D	Leaf N concentration	percent
MDAP	Physiological maturity (R7) day	DAP
P#AD	Pod number	pods m^{-2}
PD1P	Day of first pod (R3)	DAP
PWAD	Pod mass	kg ha^{-1}
$PWAD_{early}$	Pod mass for first two weeks of pod growth	kg ha^{-1}
R8AP	Harvest maturity (R8) day	DAP
$RTFD_{veg}$	Fraction root during vegetative growth	kg root kg^{-1} plant
SH%D	Shelling percentage	kg grain kg^{-1} pod
$SH\%D_{harv}$	Shelling percentage at harvest	kg grain kg^{-1} pod
SHND	Shell N concentration	percent
SLAD	Specific leaf area	cm^2 g^{-1}
SN%D	Stem N concentration	percent
$STFD_{rep}$	Fraction stem during reproductive growth	kg stem kg^{-1} shoot
$STFD_{veg}$	Fraction stem during vegetative growth	kg stem kg^{-1} shoot

†DAP, days after planting

Table 1-8. Grouping of parameters in order of optimization, minimum (Θ_p^{min}), maximum (Θ_p^{max}), initial (Θ_p^{init}), and step standard deviation (σ_p^{step}) values and literature sources for cultivar parameters estimated based on optimization with the Indore, Madhya Pradesh, India 2003 data set.

Group	Parameter	Θ_p^{min}	Θ_p^{max}	Θ_p^{init}	σ_p^{step}	Crop data	Source
1	PL-EM	2.7	11.2	5.00	0.38	EDAP	Lawn and Troedson (1990); Ranganathan et al. (2001)
2	EM-FL	10.7	60.0	46.0	1.30	ADAP	Carberry et al. (2001);
	CSDL	11.00	14.00	12.5	0.05		Chauhan et al. (2002);
	PPSEN	0.12	1.00	0.56	0.014		Prasad (1996)
3	FL-SH	2.5	22.0	18.0	1.00	PD1P	Robertson et al. (2001a,b)
	R1PPO	0.189	0.504	0.500	0.020		
4	FL-SD	2.5	30.0	28.0	1.00	$GWAD_{early}$	Robertson et al. (2001a)
5	SD-PM	22.7	40.0	36.0	2.50	MDAP	
6	R7-R8	15.0	35.0	30.0	0.7	R8AP	
7	XFRT	0.60	1.00	0.80	0.015	HIAM	
8	LFMAX	0.80	1.10	1.00	0.02	CWAM	
	SLPF	0.80	0.90	0.85	0.01		
9	SDPDV	1.6	4.0	3.5	0.10	H#UM	Remanandan (1990)
10	SFDUR	22.7	40.0	29.0	2.0	HWUM, HWAM	Remanandan (1990)
	PODUR	4	24	20.0	0.6	H#AM, P#AM	
	WTPSD	0.08	0.12	0.10	0.01		

Table 1-9. Posterior mean ($\mu_{\mathrm{p}}^{\mathrm{post}}$) and standard deviation ($\sigma_{\mathrm{p}}^{\mathrm{post}}$) for parameters estimated with the Gainesville, FL 1984 data set

Parameter	Group	$\mu_{\mathrm{p}}^{\mathrm{post}}$	$\sigma_{\mathrm{p}}^{\mathrm{post}}$
PL-EM	1	5.02	2.99E-01
EM-FL	2	32.7	1.18E+01
CSDL	2	12.94	5.20E-01
PPSEN	2	0.71	2.01E-01
FL-SH	3	17.4	2.32E-01
R1PPO	3	0.435	4.01E-02
FL-SD	4	24.1	2.03E-01
SD-PM	5	37.72	2.91E+00
R7-R8	6	8.43	1.44E+00
PROLFG	7	0.256	1.87E-02
PROLFF	7	0.226	5.46E-03
NMOBMX	7	0.143	6.63E-03
NVSMOB	7	0.39	1.28E-02
PROSTG	8	0.081	7.66E-03
PROSTF	8	0.051	1.01E-03
PROSHG	9	0.122	1.51E-02
PROSHF	9	0.062	5.65E-03
SDPRO	10	0.224	6.49E-03
SDPROG	10	0.224	6.49E-03
SDPROS	10	0.224	6.49E-03
PCARSD	10	0.633	6.49E-03
TRIFL	11	0.80	8.92E-03
FL-VS	11	11.26	2.20E+00
SLAMAX	12	669.	6.94E+01
SLAMIN	12	245.	2.15E+01
XSLATM(3)	12	11.3	6.19E-01
XSLATM(4)	12	26.3	7.15E-01
YSLATM(1)	12	0.25	3.91E-02
YSLATM(2)	12	0.25	3.91E-02
YSLATM(3)	12	0.25	3.91E-02
FL-LF	12	28.87	2.80E+00
YLEAF(1)	13	0.47	1.90E-02
YLEAF(2)	13	0.48	2.87E-02
YLEAF(3)	13	0.53	2.40E-02
YLEAF(4)	13	0.46	1.49E-02
YLEAF(5)	13	0.35	4.68E-03
YLEAF(6)	13	0.35	3.28E-03
YLEAF(7)	13	0.25	3.91E-03
YLEAF(8)	13	0.20	3.57E-02
YSTEM(1)	13	0.13	1.90E-02
YSTEM(2)	13	0.17	2.87E-02

Table 1-9. (continued)

Parameter	Group	$\mu_{\mathrm{p}}^{\mathrm{post}}$	$\sigma_{\mathrm{p}}^{\mathrm{post}}$
YSTEM(3)	13	0.17	2.40E-02
YSTEM(4)	13	0.29	1.49E-02
YSTEM(5)	13	0.45	4.68E-03
YSTEM(6)	13	0.45	3.28E-03
YSTEM(7)	13	0.55	3.91E-03
YSTEM(8)	13	0.60	3.57E-02
XFRT	14	0.99	8.51E-03
FRLFF	15	0.05	7.42E-03
FRSTMF	15	0.75	7.42E-03
SENRTE	15	0.94	6.19E-02
ICMP	15	1.75	6.35E-02
PORPT	15	0.12	1.63E-02
LFMAX	16	1.10	1.18E-03
SDPDV	17	3.89	9.52E-02
THRSH	18	76.2	2.01E+00
SFDUR	19	24.6	2.03E-01
PODUR	19	17.3	1.44E+00
WTPSD	19	0.19	6.03E-03

Table 1-10. Posterior mean ($\mu_{\mathrm{p}}^{\mathrm{post}}$) and standard deviation ($\sigma_{\mathrm{p}}^{\mathrm{post}}$) for parameters estimated with the Indore, Madhya Pradesh, India 2003 data set

Parameter	Group	$\mu_{\mathrm{p}}^{\mathrm{post}}$	$\sigma_{\mathrm{p}}^{\mathrm{post}}$
PL-EM	1	4.88	3.00E-01
EM-FL	2	29.3	1.02E+01
CSDL	2	11.60	3.09E-01
PPSEN	2	0.74	1.50E-01
FL-SH	3	9.1	4.29E+00
R1PPO	3	0.350	1.05E-01
FL-SD	4	25.8	1.85E-01
SD-PM	5	29.01	4.90E+00
R7-R8	6	22.51	4.88E+00
XFRT	7	0.70	5.93E-02
LFMAX	8	1.06	4.61E-02
SLPF	8	0.88	2.49E-02
SDPDV	9	1.81	9.06E-02
WTPSD	10	0.10	1.59E-03
PODUR	10	18.0	2.55E+00
SFDUR	10	23.4	1.12E+00

REFERENCES

Boote, K.J., Jones, J.W., Hoogenboom, G., 1998a. Simulation of crop growth: CROPGRO model, in: Peart, R.M., Curry, R.B. (Eds.), Agricultural Systems Modeling and Simulation. Marcel Dekker, Inc., New York, pp. 651–692.

Boote, K.J., Jones, J.W., Hoogenboom, G., Pickering, N.B., 1998b. The CROPGRO model for grain legumes, in: Tsuji, G.Y., Hoogenboom, G., Thornton, P.K. (Eds.), Understanding Options for Agricultural Production. Kluwer Academic Publishers, Dordecht, The Netherlands, pp. 99–128.

Boote, K.J., Mínguez, M.I., Sau, F., 2002. Adapting the CROPGRO legume model to simulate growth of faba bean. Agron. J. 94, 743–756.

Boote, K.J., Scholberg, J.M.S., 2006. Developing, parameterizing, and testing of dynamic crop growth models for horticultural crops, in: III International Symposium on Models for Plant Growth, Environmental Control and Farm Management in Protected Cultivation 718, pp. 23–34.

Brakke, M.P., 1984. Physiological aspects of pigeonpea (Cajanus cajan (L.)) growth. Master's thesis. University of Florida. Gainesville, FL.

Carberry, P.S., Ranganathan, R., Reddy, L.J., Chauhan, Y.S., Robertson, M.J., 2001. Predicting growth and development of pigeonpea: flowering response to photoperiod. Field Crops Res. 69, 151–162.

Casella, G., George, E.I., 1992. Explaining the Gibbs sampler. Am. Stat. , 167–174.

Chauhan, Y., Johansen, C., Moon, J., Lee, Y., Lee, S., 2002. Photoperiod responses of extra-short-duration pigeonpea lines developed at different latitudes. Crop Sci. 42, 1139–1146.

Chib, S., Greenberg, E., 1995. Understanding the metropolis-hastings algorithm. Am. Stat. , 327–335.

Devries, J.D., Bennett, J.M., Albrecht, S.L., Boote, K.J., 1989a. Water relations, nitrogenase activity and root development of three grain legumes in response to soil water deficits. Field Crops Res. 21, 215–226.

Devries, J.D., Bennett, J.M., Boote, K.J., Albrecht, S.L., Maliro, C.E., 1989b. Nitrogen accumulation and partitioning by three grain legumes in response to soil water deficits. Field Crops Res. 22, 33–44.

Gijsman, A., Jagtap, S., Jones, J., 2003. Wading through a swamp of complete confusion: how to choose a method for estimating soil water retention parameters for crop models. Eur. J. Agron. 18, 77–106.

Gijsman, A.J., Hoogenboom, G., Parton, W.J., Kerridge, P.C., 2002. Modifying DSSAT crop models for low-input agricultural systems using a soil organic matter-residue module from CENTURY. Agron. J. 94, 462–474.

Jones, J.W., Hoogenboom, G., Porter, C.H., Boote, K.J., Batchelor, W.D., Hunt, L.A., Wilkens, P.W., Singh, U., Gijsman, A.J., Ritchie, J.T., 2003. The DSSAT cropping system model. Eur. J. Agron. 18, 235–265.

Lawn, R.J., Troedson, R.J., 1990. Pigeonpea: physiology of yield formation, in: Nene, Y.L., Hall, S.D., Sheila, V.K. (Eds.), The pigeonpea, pp. 179–208.

Lopez, F., Setter, T., McDavid, C., 1988. Photosynthesis and water vapor exchange of pigeonpea leaves in response to water deficit and recovery. Crop Sci. 28, 141–145.

Lopez, F.B., Chauhan, Y.S., Johansen, C., 1997. Effects of timing of drought stress on leaf area development and canopy light interception of short-duration pigeonpea. J. Agron. Crop Sci. 178, 1–7.

Maliro, C.E., 1987. Physiological aspects of yield among four legume crops under two water regimes. Master's thesis. University of Florida. Gainesville, FL.

Pande, S., Gupta, R., Dahiya, S., Chauhan, Y., Singh, S., Singh, U., Jat, M., Singh, S., Sharma, H., Rao, J., Chandna, P., 2006. Reintroduction of Extra Short Duration Pigeonpea (ICPL 88039) in Rice-Wheat Cropping Systems of the Indo-Gangetic Plains. RWC Technical Bulletin No. 9. RWC-ICRISAT, NASC Complex Pusa, New Delhi.

Pathak, T., Jones, J., Fraisse, C., Wright, D., Hoogenboom, G., 2012. Uncertainty analysis and parameter estimation for the CSM-CROPGRO-Cotton model. Agronomy Journal 104, 1363–1373.

Prasad, K.L.N., 1996. Analysis of genotype X environment interaction in pigeonpea (*Cajanus cajan* (L.) Millsp.) subjected to waterlogging. Master's thesis. Andhra Pradesh Agricultural University. Hyderabad, India.

Ranganathan, R., Chauhan, Y.S., Flower, D.J., Robertson, M.J., Sanetra, C., Silim, S.N., 2001. Predicting growth and development of pigeonpea: leaf area development. Field Crops Res. 69, 163–172.

Remanandan, P., 1990. Pigeonpea: genetic resources, in: Nene, Y.L., Hall, S.D., Sheila, V.K. (Eds.), The pigeonpea, pp. 89–115.

Robertson, M.J., Carberry, P.S., Chauhan, Y.S., Ranganathan, R., O'Leary, G.J., 2001a. Predicting growth and development of pigeonpea: a simulation model. Field Crops Res. 71, 195–210.

Robertson, M.J., Silim, S., Chauhan, Y.S., Ranganathan, R., 2001b. Predicting growth and development of pigeonpea: biomass accumulation and partitioning. Field Crops Res. 70, 89–100.

Sanetra, C.M., Ito, O., Virmani, S.M., Vlek, P.L.G., 1998. Remobilization of nitrogen from senescing leaves of pigeonpea (cajanus cajan (l.) millsp.): genotypic differences across maturity groups? J. Exp. Bot. 49, 853–862.

Scholberg, J.M.S., Boote, K.J., Jones, J.W., McNeal, B.L., 1997. Adaptation of the CROPGRO model to simulate the growth of field-grown tomato, in: Kropff, M.J., Teng, P.S., Aggarwal, P.K., Bouma, J., Bouman, B.A.M., Jones, J.W., van Laar, H.H. (Eds.), Systems Approaches for Sustainable Agricultural Development: Applications of Systems Approaches at the Field Level. Kluwer Academic Publishers, London, pp. 133–151.

Sharma, D., Saxena, K.B., 1983. Genetic analysis of some leaf characteristics in pigeonpea [cajanus cajan (l.) millsp.]. Field Crops Res. 7, 257–263.

Troedson, R.J., Wallis, E.S., Singh, L., 1990. Pigeonpea: adaptation, in: Nene, Y.L., Hall, S.D., Sheila, V.K. (Eds.), The pigeonpea, pp. 159–177.